

University of Dundee

## Extreme suppression of lateral floret development by a single amino acid change in the VRS1 transcription factor

Sakuma, Shun; Lundqvist, Udda; Kakei, Yusuke; Thirulogachandar, Venkatasubbu; Suzuki, Takako; Hori, Kiyosumi

*Published in:*  
Plant Physiology

*DOI:*  
[10.1104/pp.17.01149](https://doi.org/10.1104/pp.17.01149)

*Publication date:*  
2017

*Document Version*  
Peer reviewed version

[Link to publication in Discovery Research Portal](#)

### *Citation for published version (APA):*

Sakuma, S., Lundqvist, U., Kakei, Y., Thirulogachandar, V., Suzuki, T., Hori, K., Wu, J., Tagiri, A., Rutten, T., Koppolu, R., Shimada, Y., Houston, K., Thomas, W. T. B., Waugh, R., Schnurbusch, T., & Komatsuda, T. (2017). Extreme suppression of lateral floret development by a single amino acid change in the VRS1 transcription factor. *Plant Physiology*, 175(4), 1720-1731. <https://doi.org/10.1104/pp.17.01149>

### General rights

Copyright and moral rights for the publications made accessible in Discovery Research Portal are retained by the authors and/or other copyright owners and it is a condition of accessing publications that users recognise and abide by the legal requirements associated with these rights.

- Users may download and print one copy of any publication from Discovery Research Portal for the purpose of private study or research.
- You may not further distribute the material or use it for any profit-making activity or commercial gain.
- You may freely distribute the URL identifying the publication in the public portal.

### Take down policy

If you believe that this document breaches copyright please contact us providing details, and we will remove access to the work immediately and investigate your claim.

1 **Running Title:** *deficiens* barley

2

3 **Corresponding author details:**

4 Shun Sakuma, Leibniz Institute of Plant Genetics and Crop Plant Research  
5 (IPK), Corrensstr. 3, OT Gatersleben, D-06466 Stadt Seeland, Germany. Phone:  
6 +49 39482 5-519, Email: sakuma@ipk-gatersleben.de

7 Takao Komatsuda, Institute of Crop Science, National Agriculture and Food  
8 Research Organization (NARO), Kannondai 2-1-2, Tsukuba 305 8518 Japan.  
9 Phone: +81 29-838-7408, E-mail: takao@affrc.go.jp

**Extreme suppression of lateral floret development by a single amino acid change in the VRS1 transcription factor**

Shun Sakuma<sup>1, 2, 3\*</sup>, Udda Lundqvist<sup>4</sup>, Yusuke Kakei<sup>5</sup>, Venkatasubbu Thirulogachandar<sup>2</sup>, Takako Suzuki<sup>6</sup>, Kiyosumi Hori<sup>1, 7</sup>, Jianzhong Wu<sup>1, 7</sup>, Akemi Tagiri<sup>1</sup>, Twan Rutten<sup>2</sup>, Ravi Koppolu<sup>2</sup>, Yukihisa Shimada<sup>5</sup>, Kelly Houston<sup>8</sup>, William T. B. Thomas<sup>8</sup>, Robbie Waugh<sup>8, 9</sup>, Thorsten Schnurbusch<sup>2</sup>, Takao Komatsuda<sup>1, 7\*</sup>

<sup>1</sup>National Institute of Agrobiological Sciences (NIAS), Kannondai 2-1-2, Tsukuba 305 8602 Japan; <sup>2</sup>Leibniz Institute of Plant Genetics and Crop Plant Research (IPK), Corrensstr. 3, OT Gatersleben, D-06466 Stadt Seeland, Germany; <sup>3</sup>Faculty of Agriculture, Tottori University, Koyama-Minami 4-101, Tottori 680 8550, Japan; <sup>4</sup>Nordic Genetic Resource Center (NordGen), SE-23053 Alnarp, Sweden; <sup>5</sup>Yokohama City University, Maioka 640-12, Yokohama 244 0813, Japan; <sup>6</sup>Agricultural Research Department, Hokkaido Research Organization, Chuo Agricultural Experiment Station, Higashi 6, Kita 15, Naganuma, Hokkaido 069 1395, Japan; <sup>7</sup>Institute of Crop Science, National Agriculture and Food Research Organization (NARO), Kannondai 2-1-2, Tsukuba 305 8518 Japan; <sup>8</sup>The James Hutton Institute, Invergowrie, Dundee DD2 5DA, UK, <sup>9</sup>Division of Plant Sciences, University of Dundee, Dundee DD1 4HN

**\*Corresponding authors:**

Shun Sakuma: [sakuma@ipk-gatersleben.de](mailto:sakuma@ipk-gatersleben.de)

Takao Komatsuda: [takao@affrc.go.jp](mailto:takao@affrc.go.jp)

**One sentence summary:**

Extreme suppression of lateral floret development in *deficiens* barley is the result of a single amino acid substitution in the homeodomain-leucine zipper class I transcription factor VRS1.

**Author contributions:**

S.S. and T.K. designed research. S.S., U.L., and R.K. analyzed mutants. S.S., T. Suzuki, K.Hori, and J.W. carried out the fine mapping. S.S. and A.T. performed RNA in situ hybridization and qRT-PCR. S.S., Y.K., V.T., and Y.S. analyzed RNA-seq data. S.S. and T.R. performed SEM analysis. K.Houston analyzed the

44 European Winter barely accessions. S.S., W.T., R.W., T. Schnurbusch, and T.K.  
45 wrote the manuscript. All authors have reviewed and commented on the  
46 manuscript. The authors declare no conflict of interest.

47

48 **Funding information:**

49 This research was funded by the Ministry of Agriculture, Forestry, and Fisheries  
50 of Japan (Genomics for Agricultural Innovation grants no. TRS1002 to T.K. and  
51 S.S.); a Grant-in-Aid from the Japan Society for the Promotion of Science  
52 (JSPS) Postdoctoral Fellow for Research Abroad (to S.S.); a Grant-in-Aid for  
53 Young Scientists (B) (no. 16K18635 to S.S.). The field trials work was conducted  
54 under a work package of the EU FP7 'Improving nutrient use efficiency in major  
55 European food, feed and biofuel crops to reduce negative environmental  
56 impacts of crop production' (NUE Crops) - EU-FP7 222-645 (2009 - 2014) led by  
57 Carlo Leifert of the University of Newcastle.

58   **Abstract**

59   Increasing grain yield is an endless challenge for cereal crop breeding. In barley,  
60   grain number is mainly controlled by *Six-rowed spike 1* (*Vrs1*) that encodes a  
61   homeodomain leucine zipper class I transcription factor. However, little is known  
62   about the genetic basis of grain size. Here we show that extreme suppression of  
63   lateral florets contributes to enlarged grains in *deficiens* barley. Through a  
64   combination of fine mapping and resequencing *deficiens* mutants we have  
65   identified that a single amino acid substitution at a putative phosphorylation site  
66   in *VRS1* is responsible for the *deficiens* phenotype. *deficiens* mutant alleles  
67   confer an increase in grain size, reduction in plant height and a significant  
68   increase in thousand grain weight in contemporary cultivated germplasm.  
69   Haplotype analysis revealed that barley carrying the *deficiens* allele (*Vrs1.t1*)  
70   originated from two-rowed types carrying the *Vrs1.b2* allele, predominantly  
71   found in germplasm from Northern Africa. *In situ* hybridization of *histone H4*, a  
72   marker for cell cycle or proliferation, showed weaker expression in the lateral  
73   spikelets compared to central spikelets in *deficiens*. Transcriptome analysis  
74   revealed that a number of *histone* superfamily genes were upregulated in the  
75   *deficiens* mutant suggesting that enhanced cell proliferation in the central  
76   spikelet may contribute to larger grains. Our data suggest that grain yield can be  
77   improved by suppressing the development of specific organs that are not  
78   positively involved in sink/source relationships.

## Introduction

The domestication of cereal crops such as rice (*Oryza sativa* L.), maize (*Zea mays* L.) and barley (*Hordeum vulgare* L.) began about 10,000 years ago (Doebley et al., 2006). Throughout domestication, plant forms have changed to produce larger edible parts, reduced seed dormancy and loss of shattering (Doebley et al., 2006). Together with these changes some unnecessary organs such as long barbed awns in rice (Hua et al., 2015) and high tillering in maize (Studer et al., 2011) have been lost, resulting in higher grain yields. Grain yield is affected by inflorescence architecture in cereal plants such as rice, maize, barley and wheat (*Triticum aestivum* L.) (Komatsuda et al., 2007; Shomura et al., 2008; Wang et al., 2012; Bommert et al., 2013; Koppolu et al., 2013; Poursarebani et al., 2015). In rice, a model grass plant, several major quantitative trait loci (QTLs) related to grain size such as *GW2*, *qSW5*, *GS5*, *OsSPL16* and *An-1* have been identified (Song et al., 2007; Shomura et al., 2008; Li et al., 2011; Wang et al., 2012; Luo et al., 2013). However, little is known about the genetic basis of grain size in Triticeae species including economically important crops such as wheat, barley and rye (*Secale cereale* L.), except for *TaGW2-A1*, which is a rice *GW2* ortholog in wheat (Simmonds et al., 2016) and *HvDEP1* in barley, an orthologue of rice *Dense and Erect Panicle 1* (Wendt et al., 2016).

As a model organism for plant development in the Triticeae, barley has been useful due to its simple diploid genome and the availability of a large number of different morphological mutants (Druka et al., 2011). In the genus *Hordeum*, including cultivated barley, the inflorescence is called a spike and is composed of three uni-floreted spikelets at each rachis node (Bothmer et al., 1995). When all three spikelets are fertile and produce grains the spike is called six-rowed whereas only central spikelets are fertile in a two-rowed spike. Barley row-type is one of the most important traits affecting yield, especially for grain number, and advancing its molecular understanding is therefore key to yield improvement. Row-type is controlled by at least five loci: *Six-rowed spike 1* (*vrs1* [syn=*HvHox1*]), *Six-rowed spike 2* (*vrs2*), *Six-rowed spike 3* (*vrs3*), *Six-rowed spike 4* (*vrs4*), and *Intermedium spike-c* (*int-c* [syn=*vrs5*]) and all five genes have

111 been identified (Komatsuda et al., 2007; Ramsay et al., 2011; Koppolu et al.,  
112 2013; Bull et al., 2017; van Esse et al., 2017; Youssef et al., 2017). In four of  
113 these (*Vrs1*, *Vrs2*, *Vrs4* and *Vrs5*) wild-type alleles encode transcription factors;  
114 homeodomain-leucine zipper class I (HD-Zip I), *SHORT INTERNODES* (*SHI*),  
115 *RAMOSA2* (*HvRA2*), and *TEOSINTE BRANCHED1* (*HvTB1*) respectively, and  
116 in *Vrs3* the wild-type allele putatively encodes a histone H3K9 demethylase.  
117 Loss of function at any of these five genes results in varying levels of fertile  
118 lateral spikelet development. Selection of naturally occurring six-rowed alleles of  
119 *vrs1* and *int-c* during the domestication of barley positively affected production  
120 (Komatsuda et al., 2007; Ramsay et al., 2011).

121  
122 HD-Zip I class genes like *Vrs1* have evolved through a series of gene  
123 duplications and divergence through subfunctionalization or neofunctionalization  
124 (Ariel et al., 2007; Sakuma et al., 2013). *HvHox2*, which is a paralog of *Vrs1*  
125 (*HvHox1*) is highly conserved among cereals and expressed broadly (Sakuma et  
126 al., 2010). So far, a loss-of-function mutant of *HvHox2* has not been reported;  
127 thus the gene has been considered as essential for plant development. In  
128 contrast, *Vrs1* plays more specific roles in the control of lateral spikelet fertility.  
129 *Vrs1* is expressed in the lateral florets, especially in the pistil; at least 58 loss-of  
130 function mutants have been described and it therefore seems to be a driving  
131 force of genetic variation in barley spike development (Komatsuda et al., 2007;  
132 Sakuma et al., 2013).

133  
134 *Deficiens* barley plants have a two-rowed spike with extremely rudimental lateral  
135 spikelets/florets compared with canonical two-rowed cultivars (Fig. 1A). The  
136 *deficiens* phenotype is a naturally occurring variant and potentially an allele of  
137 *Vrs1* (Habgood and Chambi, 1984). *Deficiens* barley is endemic in Ethiopia  
138 where the unique spike of *labile*, which displays a variable number of fertile  
139 spikelets at each rachis node, is also localized (Woodward, 1949; Youssef et al.,  
140 2014). Old studies report that *deficiens* barley affects the grain size of central  
141 spikelets (Powers, 1936; Habgood and Chambi, 1984). Currently, *deficiens*  
142 types dominate United Kingdom winter barley seed production, and hence the

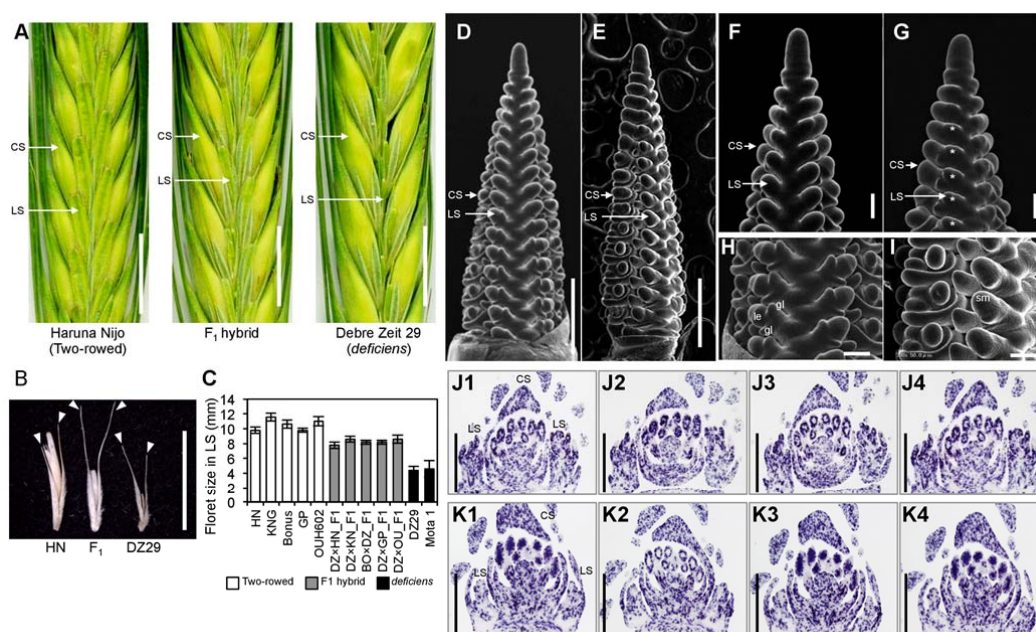


**Figure 1.** The inflorescence of *deficiens* barley.

(A) The morphology of the inflorescence (from left to right: canonical two-rowed spike cultivar Haruna Nijo, HN; F<sub>1</sub> plant between DZ29 × HN; *deficiens* landrace Debre Zeit 29, DZ29). Central spikelets of DZ29 are larger than those of HN, lateral spikelets of DZ29 are smaller than those of HN. (B) Dissected lateral spikelets. Arrowheads indicate glumes. (C) Variation of floret size in the lateral spikelet. KNG; Kanto Nakate Gold, GP; Golden Promise. (D–I) SEM images of two-rowed cultivar Bonus (D, F, H) and DZ29 (E, G, I) at the awn primordium stage. Asterisks indicate smaller lateral spikelet meristems in DZ29 compared with Bonus. (J and K) *In situ* mRNA hybridization of *histone H4* shows weaker expression in lateral spikelet of DZ29 (K) than that of Bonus (J), while stronger expression in the central spikelet (all the organs) of DZ29 than that of Bonus. Four serial sections are shown in each cultivar. Scale bars = 1 cm in (A), (B), 500 μm in (D), (E), (J), (K) and 100 μm in (F–I). CS: central spikelet; LS: lateral spikelet; gl: glume; le: lemma; sm: spikelet meristem.

area grown, and are increasing in spring barley (Fig. S1). Although breeders recognize the agricultural importance of a perceived yield advantage, the molecular genetic basis of the *deficiens* is not understood. The present study sought to identify the *deficiens* locus through positional cloning and to elucidate the molecular mechanism underlying the extreme suppression of the floral organs of lateral spikelets in barley.



## 151     **Results**

### 152     **Phenotype of *deficiens* barley**

153     *Deficiens* barley (Debre Zeit 29; DZ29) shows extremely rudimental lateral floral  
154     organs although glume development in its lateral spikelets was comparable to  
155     canonical two-rowed barley (Fig. 1A, B). To better understand the *deficiens*  
156     phenotype the size of florets in the lateral spikelets was measured at the  
157     anthesis stage in field conditions. *Deficiens* barleys produced 4–5 mm long  
158     florets in its lateral spikelets, significantly less than the 10–12 mm lengths of  
159     canonical two-rowed varieties. F<sub>1</sub> plants from five different parental crosses  
160     showed an intermediate phenotype (7–9 mm) compared with parental lines (Fig.  
161     1C) showing a low degree of dominance (0.26, 0.17, 0.23, 0.41, and 0.27, for  
162     DZ×HN, DZ×KN, BO×DZ, DZ×GP, and DZ×OU, respectively). To investigate the  
163     effect of *deficiens* on the development of lateral spikelets (especially florets) in  
164     more detail, scanning electron microscopy (SEM) images were compared (Fig.  
165     1D, E). Barley spike development progresses from the basal to apical part  
166     gradually (Kirby and Appleyard, 1981; Youssef et al., 2017). At the apical part of  
167     spike, when triple spikelet primordia had differentiated, DZ29 showed a smaller  
168     lateral spikelet meristem compared with canonical two-rowed type (Fig. 1F, G).  
169     In the canonical type, the lateral spikelet meristems have differentiated into  
170     glume and lemma primordia at the basal part, whereas those of DZ29 remained  
171     as undifferentiated spikelet meristems (Fig. 1H, I) with suppressed floral  
172     differentiation (Fig. 1D–I).

173     To explore cellular activity of the spikelet meristems, RNA *in situ* hybridization  
174     was conducted using *histone H4* antisense probe as a marker for active cell  
175     division. The results showed that the transcripts of *histone H4* were detectable in  
176     both DZ29 and canonical two-rowed barley (Fig. 1J, K, Fig. S2). Related  
177     abundance of the transcript in the lateral spikelets compared to that in the  
178     central spikelets is less in DZ29 (Fig. 1K) compared with canonical two-rowed  
179     barley (Fig. 1J) although the *in situ* hybridization is not quantitative (Fig. S2).  
180     Interestingly, stronger signals were observed in the central spikelet of DZ29,  
181     suggesting enhanced cell proliferation. These phenotypic data suggest that

182 *deficiens* causes an enduring suppression of lateral spikelet primordia from an  
183 early stage of spike development onwards.

184

#### 185 **Map-based identification of *deficiens***

186 To map the *deficiens* gene five filial generation 2 (F<sub>2</sub>) segregating populations  
187 were produced and the genotype of each F<sub>2</sub> individual was inferred by F<sub>3</sub>  
188 progeny analysis to show that the genotype segregated as a monogenic factor  
189 (Fig. S3, Table S1). Depending upon the cross, the gene was localized to within  
190 a 1.0–2.6 cM interval on chromosome 2H (Fig. S4). No recombinants with the  
191 HvHox1\_DraIII marker, defined by a SNP located on the promoter region of  
192 *HvHox1* (–359 bp from transcription start site), were observed. The marker order  
193 in the region was conserved across all five mapping populations, indicating no  
194 chromosomal rearrangements (Fig. S4).

195

196 Larger scale F<sub>2</sub> populations of 2,096 and 2,264 individuals for DZ29 × OUH602  
197 and DZ29 × KNG, respectively, refined the *deficiens* locus to a 0.02 cM region  
198 flanked by the markers e40m36-1110S\_AccIII and BC12348\_HhaI (Fig. 2A,  
199 Table S2). The interval is composed of 458,564 bp in Morex BAC sequences  
200 (accession no. EF067844) (Komatsuda et al., 2007) and only one predicted  
201 gene, *Vrs1* (*HvHox1*) encoding a homeodomain leucine zipper class I  
202 transcription factor, was found in the interval. A sequence comparison of the  
203 *Vrs1* locus (1,580 bp upstream, 1,538 bp coding region, 1,183 bp downstream)  
204 among mapping parents revealed a base pair change that encoded a single  
205 amino acid substitution (S184G: 184 serine to glycine) at the Serine-rich motif of  
206 the C-terminal region (CTR) specific to DZ29 (renamed *Vrs1.t1* allele, Fig. S5).  
207 Resequencing *Vrs1* in 48 NW European winter barley cultivars (24 canonical  
208 two-rowed and 24 *deficiens*) revealed that all 24 accessions of the *deficiens* type  
209 shared the *Vrs1.t1* allele (Table S3). Furthermore, according to the NCBI  
210 database all sequenced accessions of *deficiens* barley have an identical amino  
211 acid sequence as VRS1.t1 (Table S3). This suggests that the amino acid change  
212 in this region may be responsible for the *deficiens* phenotype.

213

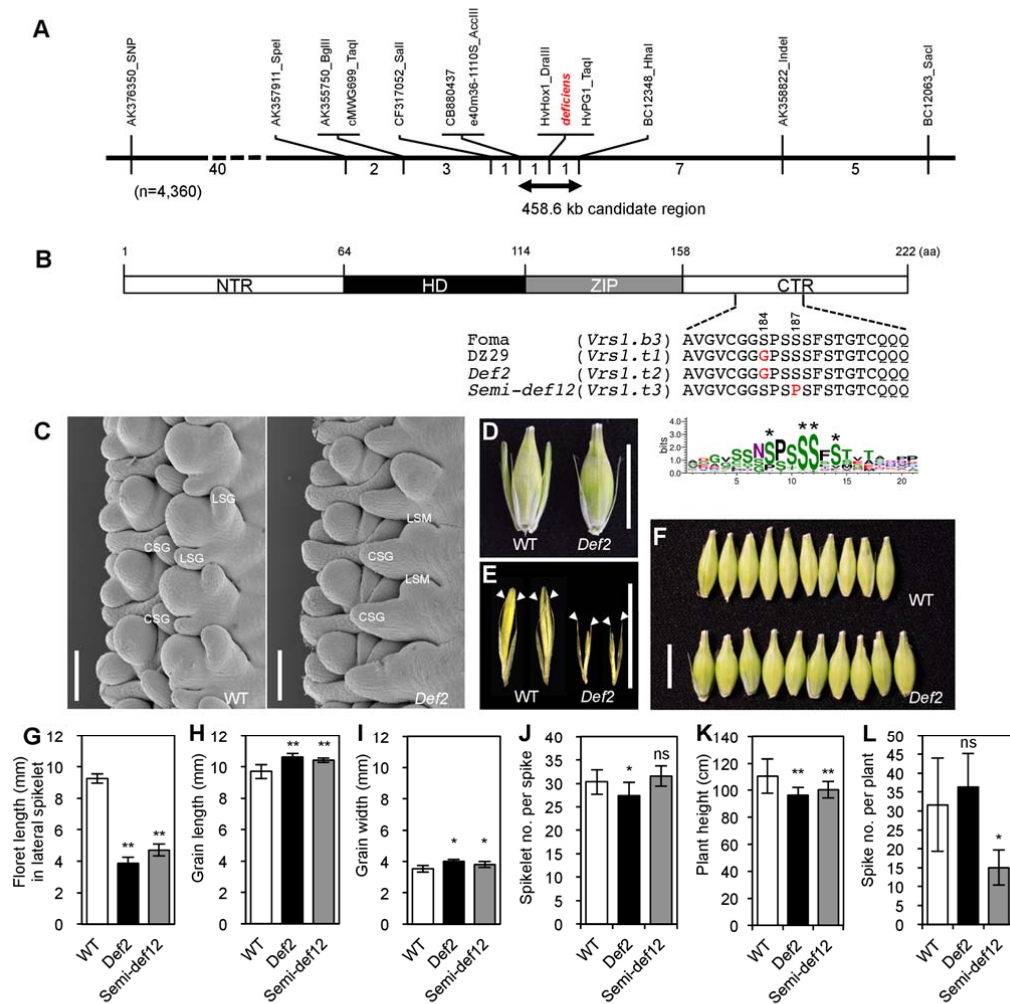


**Figure 2.** Fine mapping of *deficiens* and analysis of induced mutants.

(A) The genetic map of the *deficiens* region. The numbers beneath the line indicate the number of recombinants recovered. One recombination corresponds to a genetic distance of 0.01 cM. (B) Protein sequence of VRS1. Independent single amino acid substitutions were identified in DZ29 and induced mutants (S184G & S187P) at C-terminal region (CTR), respectively. The Ser-rich motif is highly conserved among plant HD-Zip I proteins ( $n = 87$ ). Asterisks indicate putative phosphorylation sites. NTR: N-terminal region; HD: homeodomain; ZIP: leucine zipper. (C) SEM images of Foma (WT) and *Deficiens 2* (*Def2*) mutant at awn primordium stage. In *Def2* the lateral spikelet meristem is highly suppressed. CSG: central spikelet glume; LSG: lateral spikelet glume; LSM: lateral spikelet meristem. (D) Triple spikelet morphology. (E) Dissected lateral spikelets. Arrowheads indicate glumes. (F) *Def2* mutant shows bigger grain size. (G–L) Phenotypic comparison between Foma (WT) and *deficiens* mutants. (G) floret length in the lateral spikelet, (H) grain length, (I) grain width, (J) central spikelet number per spike, (K) plant height, (L) spike number per plant. Data are given as mean  $\pm$  sd ( $n = 20$ ). \*\*, \*, Means are significantly different at the 1 and 5% probability levels, respectively; ns, not significantly different. Scale bars show 100  $\mu$ m in (C) and 1 cm in (D–F).

214 To test this hypothesis, seven *Deficiens* mutants and 35 *Semi-deficiens* mutants  
 215 derived from canonical two-rowed cultivars (Foma, Bonus, Kristina and Lina)  
 216 were phenotyped and re-sequenced (Table S4). Two of the 42 induced mutants,

217 *Deficiens 2* (*Def2*, named *Vrs1.t2* allele) and *Semi-deficiens 12* (*Semi-def12*,  
218 named *Vrs1.t3* allele) derived from cv. Foma, showed a clear *deficiens* spike  
219 phenotype with rudimentary lateral spikelets (Fig. 2C–E, G, Fig. S6). These two  
220 mutants had independent single amino acid substitutions, S184G and S187P  
221 respectively, at the CTR (Fig. 2B, Table S4) suggesting that a single amino acid  
222 substitution of serine in the Ser-rich motif was responsible for the *deficiens*  
223 phenotype (Fig. S7). The remaining 40 lines did not show a *deficiens* phenotype  
224 nor a sequence variant, suggesting that either the character has been lost from  
225 the genebank stocks or the phenotype was environmentally controlled and not  
226 genetic (Table S4). SEM images of *Def2* showed that lateral spikelet meristems  
227 seem to arise from the central spikelet glume (Fig. 2C and Fig. S8). Interestingly,  
228 the *Def2* mutant shares an identical SNP (A > G at position +775 relative to the  
229 start codon) with *deficiens* cultivars including DZ29. To date, *Vrs1* has been  
230 resequenced in more than four hundred lines but neither the nucleotide  
231 sequences (nor haplotypes) of *Def2* nor *Semi-def12* mutants were found in any  
232 databases suggesting this change is novel, originating from a mutation in cv.  
233 Foma. Interestingly, the Ser-rich motif around the position of 184 and 187 was  
234 highly conserved amongst plant HD-Zip I class transcription factors ( $n = 87$ ; 22  
235 species in Embryophyta, Fig. 2B, Table S5 and Supplementary Data 1). Since  
236 serine is known as a potential phosphorylation site, we examined the possibility  
237 of phosphorylation of serine using the program NetPhos 3.1. The results showed  
238 that the serine residues at CTR in canonical two-rowed genotypes are predicted  
239 targets of phosphorylation, whereas *deficiens* alleles showed lower potential  
240 than the threshold (Fig. S9) suggesting an altered phosphorylation status in  
241 *deficiens* lines.

242

243 To understand the phenotypic effect of the *deficiens* mutations, several  
244 agronomic traits were compared between Foma (WT) and its derived *Def2* and  
245 *Semi-def12* mutants. Both *deficiens* mutants showed about a 10% increase in  
246 grain length and width compared with WT (Fig. 2F, H, I). Moreover, both  
247 *deficiens* mutants showed reduced plant height compared with WT (Fig. 2K).

248 The significant difference of spikelet number per spike was only observed in  
249 *Def2* and spike number per plant in *Semi-def12*.

250

251 The phenotypic effect of *deficiens* (*Vrs1.t1*) was then assessed in the collection  
252 of 48 contemporary North West European winter barley cultivars (24 canonical  
253 two-rowed and 24 *deficiens*) referred to previously for yield and yield related  
254 traits (Figure 3). The *deficiens* lines have a significantly higher thousand grain  
255 weight (56.5 g) than the canonical two-rowed lines (53.5 g) (t (23),  $p=0.002$ ). In  
256 this set of germplasm the number of spikes per m<sup>2</sup> was slightly, but not  
257 significantly, lower for the *deficiens* lines (629.8) compared to two-rowed lines  
258 (665.3) (t (23),  $p=0.051$ ) and *deficiens* does not significantly influence yield  
259 (*deficiens* = 7.2 t/ha, two-rowed = 7.1 t/ha) or grains per spike (*deficiens* = 20.5,  
260 two-rowed = 20.1).

261

#### 262 **Expression pattern of *Vrs1* in *Deficiens 2* mutant**

263 Quantifying mRNA levels at different developmental stages revealed no  
264 significant differences in *Vrs1* transcript abundance at the beginning of spike  
265 development (from double-ridge to lemma primordium stage) between WT and  
266 *Def2* mutant. This indicates that *Vrs1* is normally regulated at this stage (Fig. 4A).  
267 After the lemma primordium stage, however, the *Vrs1* transcript level was  
268 significantly decreased in both *Def2* (Fig. 4A) and DZ29 (Fig. S10). To determine  
269 whether or not the reduced *Vrs1* transcript level was affected by the upstream  
270 regulator *Vrs4*, we examined *Vrs4* expression levels but found no significant  
271 difference between WT and *Def2* (Fig. 4B). The expression pattern of *HvHox2*,  
272 which is a paralog of *Vrs1*, was also not significantly different (Fig. 4C).

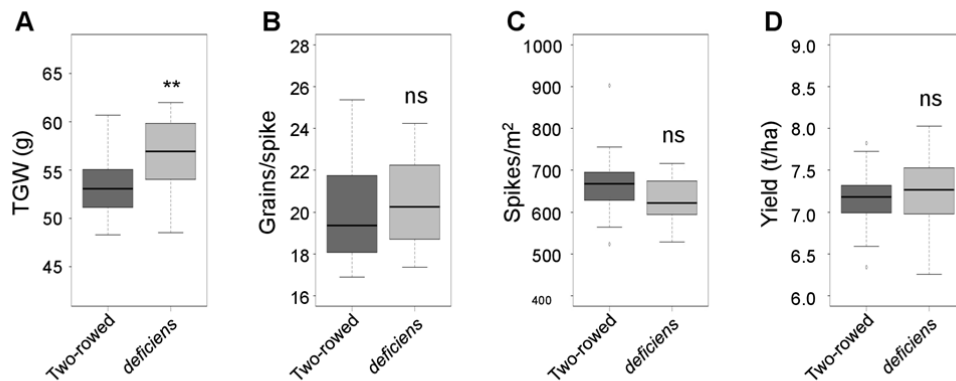


**Figure 3.** Mean effect of *deficiens* allele for grain yield. (A) Thousand grain weight (TGW). (B) Grains per spike. (C) Spikes per m<sup>2</sup>. (D) Yield (t/ha). Data were obtained from 5 site/seasons field trial of 24 two-rowed and 24 *deficiens* NW European cultivars grown under a winter feed barley regime (200kg total N/ha). \*\*, \*, Means are significantly different at the 1 and 5% probability levels, respectively; ns, not significantly different.

273 The hypothesis that a different tissue localization of the *Vrs1* transcript could  
 274 also be responsible for the *deficiens* phenotype guided us to test this possibility  
 275 by RNA *in situ* hybridization using *Vrs1* specific probes (Sakuma et al., 2013).  
 276 *Vrs1* mRNA was clearly localized to the lateral spikelet meristem in both  
 277 *deficiens* and canonical two-rowed barley at the glume primordium stage and the  
 278 white anther stage respectively (Fig. 4D–G). These qRT-PCR and *in situ*  
 279 hybridization data suggest that the amino acid alterations of VRS1, but not  
 280 mRNA differences, were responsible for the *deficiens* phenotype.

281

## 282 **Genome-wide transcriptional regulation by *Deficiens 2***

283 To identify the transcriptional changes underlying the morphological differences  
 284 during immature spike development, RNA-seq was conducted using developing  
 285 spikes at the awn primordium stage of both WT and the *Def2* mutant. Based on  
 286 SEM analysis at this developmental stage the meristem of the lateral spikelet  
 287 remains undifferentiated in *Def2* (Fig. 2C). We reasoned that such a clear  
 288 morphological difference should enable the detection of differentially expressed  
 289 genes (DEGs). RNA-seq analysis revealed 1,256 DEGs ( $q$ -value < 0.05,  $p$ -value  
 290 < 0.05 and log<sub>2</sub> fold change > 1 or < -1); comprised of 860 (68.5%) upregulated  
 291 and 396 (31.5%) downregulated genes in the *Def2* mutant relative to WT (Fig.  
 292 5A, Table S6). Gene Ontology (GO) enrichment analysis of the differentially

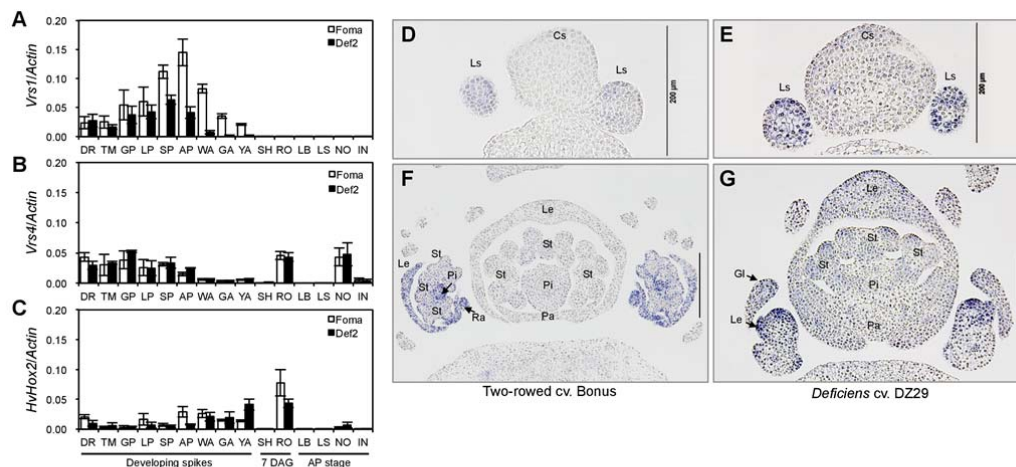


**Figure 4.** Transcript pattern of *Vrs1*, *Vrs4* and *HvHox2*.

(A–C) Quantitative real time PCR comparison of *Vrs1* (A), *Vrs4* (B), and *HvHox2* (C) in selected tissues between Foma and *Deficiens 2* mutant. DR: double ridge stage; TM: triple-mound stage; GP: glume primordium stage; LP: lemma primordium stage; SP: stamen primordium stage; AP: awn primordium stage; WA: white anther stage; GA: green anther stage; YA: yellow anther stage; SH: shoots; RO: roots; LB: leaf blade; LS: leaf sheath; NO: nodes; IN: internodes. (D–G) *In situ* mRNA hybridization with *Vrs1* antisense probe. *Vrs1* is predominantly expressed in the lateral spikelet meristem at the glume primordium stage of Bonus (*Vrs1.b3*, D) and DZ29 (*Vrs1.t1*, E). At the white anther stage, *Vrs1* is mainly localized in lemma, pistil and rachilla in Bonus (F) whereas *Vrs1* is expressed in floret meristem and lemma primordia in DZ29 (G). Cs: central spikelet; Ls: lateral spikelet; Gl: glume; Le: lemma; St: stamen; Pi: pistil; Ra: rachilla. Scale bars show 200 μm.

expressed genes revealed that genes upregulated in *Def2* (Supplementary Data 3) were highly enriched for molecular functions related to DNA binding (GO:0003677,  $P = 5.80e-11$ ) and glutathione transferase activity (GO:0004364,  $P = 1.20e-10$ ) (Fig. 5B and Table S7). The DNA binding class includes 78 *histone* superfamily genes, indicating promotion of cell proliferation in *Def2*; this might be related with the fact that grain size was increased in *deficiens* alleles (Fig. 2). In contrast, genes downregulated in *Def2* were not generally enriched for any GO terms (Supplementary Data 4), although we did detect downregulation of cytokinin oxidase/dehydrogenase (*CKX*) genes, which are involved in cytokinin degradation (HORVU3Hr1G105360 and HORVU3Hr1G075920). Reduced expression of *CKX* gene generally causes cytokinin accumulation and more meristem activity (Ashikari et al., 2005; Han et al., 2014). The reduction of *Vrs1* (HORVU2Hr1G092290) expression level in *Def2* was also detected in RNA-seq analysis, which validates the findings of the qRT-PCR experiment.

## The origin of *deficiens* barley



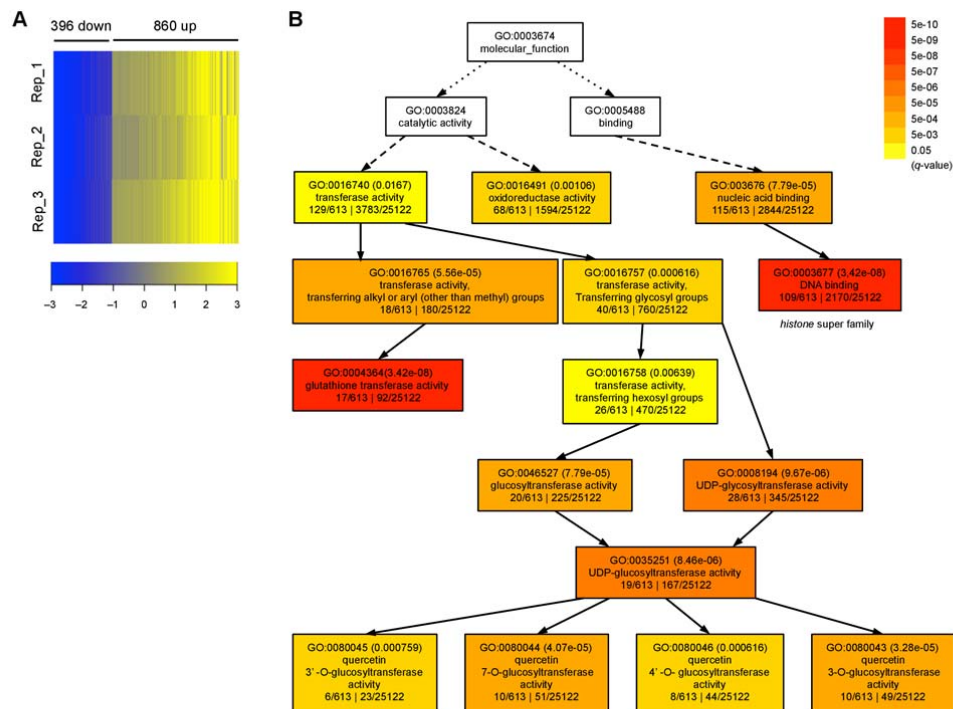


**Figure 5.** Transcriptional regulation by the *Deficiens* mutation. (A) Heat map of differentially expressed genes (DEG) in *Def2* mutant (*Vrs1.t2* allele) compared with Foma. (B) Hierarchical tree graph of Gene Ontology (GO) enrichment for the up-regulated DEG. Numbers in parentheses indicate *q*-values. Solid, dashed, and dotted lines represent two, one and zero enriched terms at both ends connected by the line, respectively.

310 The *deficiens* landraces are predominantly distributed in Ethiopia and a  
 311 monophyletic origin of *deficiens* is hypothesized. To infer the origin of the  
 312 *deficiens* allele (*Vrs1.t1*), we reanalyzed the sequence of the *Vrs1* region (2062  
 313 bp length) from 321 domesticated barley and 136 wild barley accessions (Saisho  
 314 et al., 2009). Haplotype network analysis revealed that *Vrs1.t1* allele (Haplotype  
 315 10) was derived from the *Vrs1.b2* allele (Haplotype 6) through a single  
 316 nucleotide substitution in exon 3, which resulted in the S184G amino acid  
 317 substitution implying that *Vrs1.b2* was the immediate ancestral allele of *Vrs1.t1*



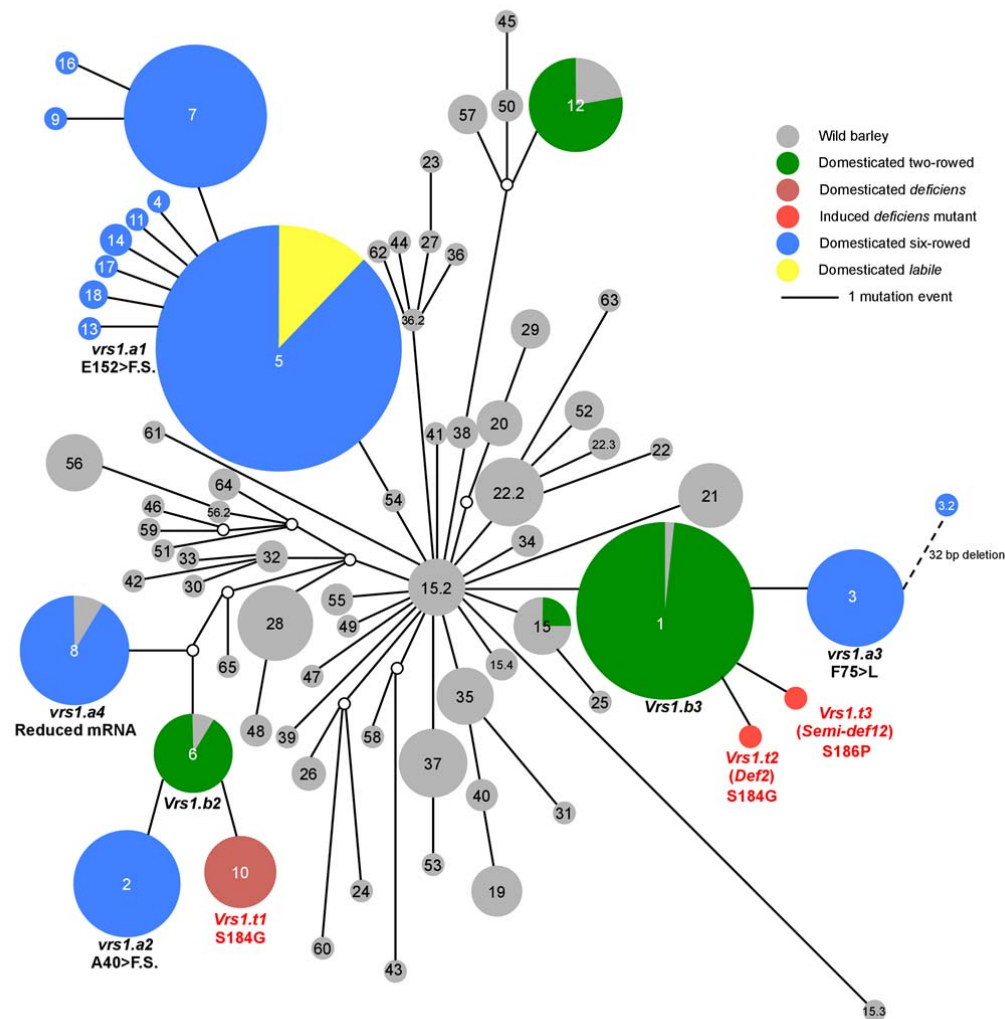


**Figure 6.** Haplotype network analysis of *Vrs1*.

Median-Joining network was constructed from the haplotypes based on the re-sequencing of 321 domesticated and 136 wild barley accessions. Circle sizes correspond to the frequency of individual haplotypes. Lines represent genetic distances between haplotypes. Open circle indicate inferred intermediate haplotypes.

(Fig. 6). Landraces carrying Haplotype 6 are predominantly distributed in North Africa (Table S8). Interestingly, the *vrs1.a2* allele (Haplotype 2), a six-rowed spike, was also derived from the same *Vrs1.b2* allele through a single nucleotide insertion in exon 2, which results in a frame shift of the amino acid sequence (A40>F.S.; Fig. 6). Landraces carrying the *vrs1.a2* allele are distributed throughout North Africa, South Europe and North America. Both *Vrs1.t1* (contributing grain size) and *vrs1.a2* (contributing grain number) alleles originated from North Africa. While *Vrs1.t1* was endemic to Ethiopia, *vrs1.a2*

326 expanded to North Africa and South Europe. We consider it remarkable that the  
327 opposite yield components, grain size and grain number, are controlled by  
328 different alleles derived from the same *Vrs1* gene and ancient people selected  
329 both mutations independently.

330

331 Considering contemporary North West European winter cultivars, we identified 3  
332 SNPs in the CDS of *Vrs1* leading to amino acid substitutions, D8G, D26E,  
333 S184G, and one SNP in the 2<sup>nd</sup> intron of this gene (Table S3). These 4 SNPs are  
334 in complete linkage disequilibrium, and the two haplotypes segregate based on  
335 the canonical two-rowed/*deficiens* phenotype of each cultivar. All of the *deficiens*  
336 lines contain the *Vrs1.t1* allele, shared with accessions originating from Ethiopia  
337 (Table S3).

338

339

## 340 **Discussion**

### 341 **A single amino acid substitution in VRS1 is responsible for *deficiens*** 342 **barley**

343 *Deficiens* has previously been considered one of the multiple alleles at the *Vrs1*  
344 locus (Woodward, 1947), but its causal mutation had not been discovered. In the  
345 present study, detailed phenotypic observation confirmed that *deficiens* alleles  
346 extremely suppress floret development in the lateral spikelets. Our genetic  
347 analysis strongly suggests that a point mutation leading to a single amino acid  
348 substitution at the conserved Ser-rich motif in C-terminal region (Motif 4) of  
349 VRS1 is responsible for the developmental fate of the lateral spikelet. This  
350 Ser-rich motif is highly conserved among plant HD-Zip I class transcription  
351 factors but its biological function(s) remained elusive. Next to threonine and  
352 tyrosine, serine is an amino acid residue commonly phosphorylated by several  
353 kinases in eukaryotes. Large-scale phosphorylation mapping analysis revealed  
354 85% of serine residues in Arabidopsis to be phosphoserine (Sugiyama et al.,  
355 2008). Phosphorylation influences the stability and activity of transcription  
356 factors (Hunter and Karin, 1992; Fujiwara et al., 2008). When phosphorylated,  
357 CONSTANS (CO), a flowering promoter encoding a B-box zinc finger, influences  
358 the rate of turnover of the CO protein via activity of the CONSTITUTIVE  
359 PHOTOMORPHOGENIC 1 (COP1) ubiquitin ligase (Sarid-Krebs et al., 2015).  
360 Phosphorylated CONSTANS is the preferred substrate for degradation. In this  
361 study, almost all serine residues in the Ser-rich motif (Motif 4) were predicted as  
362 phosphoserine in the canonical two-rowed allele of *Vrs1* but not in its *deficiens*  
363 alleles because of a single amino acid substitution in Motif 4. From our results,  
364 we hypothesize that hypo-phosphorylated VRS1 in *deficiens* remains functional  
365 for longer during a critical stage in plant development, resulting in stronger  
366 suppression of floret development in the lateral spikelets. The expression  
367 analysis revealed that the *deficiens* phenotype is not due to an overexpression  
368 of *Vrs1* but most likely acts at the protein level (Fig. 4). Reduced *Vrs1* transcript  
369 levels from the stamen primordium stage onwards are probably due to the much  
370 smaller size of the lateral spikelets, compared with WT, noting that *Vrs1* mRNA is  
371 predominantly localized in the lateral spikelets (Fig. 4D–G).

372

373 Since *Vrs1* evolved through gene duplication and neofunctionalization, the  
374 mutation frequency is notably higher than in its paralog *HvHox2* (Sakuma et al.,  
375 2010; Sakuma et al., 2013). Six of the 58 *vrs1* mutants identified so far have a  
376 mutation at the C-terminal region (Motif 4 end and motif 10 in this study), which  
377 is considered as a transcriptional activation domain (Komatsuda et al., 2007;  
378 Arce et al., 2011). This region is in the vicinity of the phosphorylation region, and  
379 the mutation sites were C194>S (*Int-d.11*), Q196>stop (*Int-d.36*), Q197>stop  
380 (*Int-d.40*) and A203>frame shift (*hex-v.27*, *hex-v.30* and *hex-v.31*). Previous  
381 yeast two hybrid assays showed that the C-terminal region (Motifs 4 and 10 in  
382 this study) of VRS1 functions as a transcriptional activator (Sakuma et al., 2013).  
383 Therefore, the six *vrs1* mutants mentioned above could each be considered to  
384 represent a loss of transactivation activity as a transcription factor. By identifying  
385 its role in the suppression of floret primordia, the present study is the first to  
386 uncover a biological function of the Ser-rich motif in HD-Zip I transcription  
387 factors.

388

### 389 **Higher yield potential of *deficiens* barley**

390 *Deficiens* is now the major spike type of winter barleys grown in NW Europe, and  
391 is increasing in the European spring barley crop (Fig. S1). We therefore  
392 hypothesize that *deficiens* spike types have replaced canonical two-rowed types  
393 due to a higher grain yield potential associated with the altered spike  
394 architecture. Our results strongly support this hypothesis since two independent  
395 mutant accessions showed enlarged grains, which is positively related to higher  
396 grain yield. It is hard to think of why *deficiens* resulted in reduced height; though  
397 a possible explanation is a change in resource partitioning or additional  
398 mutations at other loci that reduce height. A previous study showed that the  
399 sterile lateral spikelets of canonical two-rowed barleys do not contribute to  
400 photosynthesis suggesting that there is potential conflict between the central  
401 and lateral spikelets for assimilate supply (Habgood and Chambl, 1984). The  
402 notion that *vrs1* loss-of-function mutants produce more but smaller-grains  
403 compared to WT supports this model. Improvement of grain size could therefore

404 be achieved by suppressing the development of specific organs (in this study;  
405 lateral spikelets), which do not contribute to yield potential.

406

407 Our RNA-seq analysis revealed that a number of *histone* genes were  
408 upregulated in the *Def2* mutant suggesting active cell proliferation in the central  
409 spikelet which in turn may result in bigger grain size. This hypothesis is partially  
410 supported by the *in situ* hybridization analysis with *histone H4* probe showing  
411 higher signals in the central spikelet and lower signals in the lateral spikelet of  
412 *deficiens* barley (Fig. 1J, K). Since lateral florets were strongly suppressed at the  
413 awn primordium stage, the upregulation of *histone* genes would be a central  
414 spikelet event and an indirect effect through the suppression of lateral floret  
415 development. In rice, higher expression of *GW6a* enhances grain weight and  
416 yield by increasing acetylation levels of histone H4 and upregulation of cell cycle  
417 genes (Song et al., 2015). Interestingly, the rare allele elevating *GW6a*  
418 expression has escaped human selection during rice domestication and modern  
419 breeding. Enlarged grain size and thus TGW in *deficiens* barley, as observed in  
420 both mutant germplasm and NW European cultivars, could be analogous to the  
421 *GW6a* event in rice, albeit at an independent locus. However, the precise  
422 mechanism by which upregulating cell cycle genes pre-fertilization leads to  
423 increases in grain size remains to be established.

424

425 Haplotype network analysis revealed that both *Vrs1.t1* and *vrs1.a2* alleles  
426 originated from a point mutation of the *Vrs1.b2* allele. Based on geographical  
427 data, it stands to reason that mutation of *Vrs1.b2* to *Vrs1.t1* occurred in Ethiopia  
428 and was selected there while *vrs1.a2* was selected in North-west Africa and then  
429 distributed to Southern Europe. Remarkably, two different alleles with opposing  
430 phenotypic effects, enlarged grain size and increased grain number, were  
431 selected independently during barley domestication, presumably due to different  
432 selective forces for these two competing components of yield. *Vrs1.t1* can be  
433 considered a rare allele, and its utilization has increased in NW European winter  
434 and spring barley only recently.

435

436 In summary, we identified that the *deficiens* spike architecture of cultivated  
437 barley is the result of a single amino acid substitution in a conserved motif of the  
438 major row-type protein VRS1. The substitution leads to a repression of the  
439 development of the lateral florets on the barley spike. Our phenotypic analysis  
440 suggested that *deficiens* alleles (*Vrs1.t1*, *.t2*, and *.t3*) ultimately contribute to  
441 increasing the size of grain in the central spikelets. Haplotype analysis indicates  
442 that the natural *deficiens* *Vrs1.t1* allele originated from a point mutation in the  
443 two-rowed allele *Vrs1.b2*, an event that most probably occurred in Ethiopia.  
444 Unlocking the precise molecular cause of the *deficiens* spike morphology will  
445 enable direct selection for higher yielding two-rowed barley varieties and  
446 enhance our biological understanding of the molecular mechanisms  
447 underpinning the elaboration of barley inflorescence development.

448

## 449 **Material and Methods**

### 450 **Plant materials**

451 The *deficiens* barley (*Hordeum vulgare* var. *deficiens*) Debre Zeit 29 (DZ29,  
452 SV043) and Mota 1 (SV039) together with wild barley line OUH602 (*H. vulgare*  
453 ssp. *spontaneum*) were obtained from the Institute of Plant Science and  
454 Resources, Okayama University, Kurashiki, Okayama, Japan. Canonical  
455 two-rowed cultivars (cv.), Haruna Nijo (HN), Kanto Nakate Gold (KNG), Bonus  
456 (BO), Foma, Golden Promise (GP) were obtained from National Institute of  
457 Agrobiological Sciences (NIAS), Tsukuba, Japan. The *Deficiens* and  
458 *Semi-deficiens* mutants listed in Table S4 were obtained from the Nordic gene  
459 bank (NordGen, Alnarp, Sweden). 24 *deficiens* and 24 canonical two-rowed  
460 cultivars grown under a feed nitrogen regime were analyzed in the current paper.  
461 They were first placed on the UK National List between 1992 – 2012, and 1992 –  
462 2007 respectively, representing as far as possible a balanced dataset, and  
463 focusing on contemporary, relevant germplasm. The field trials were grown over  
464 5 site/season combinations in Scotland, England, and Germany for harvest  
465 years 2010 and 2011 with known available soil mineral nitrogen content. Each  
466 trial was supplemented with three fertilizer regimes in a split plot design with  
467 partial replication; no nitrogen application, a malting nitrogen application and a

feed nitrogen application. Plots were sown at a constant density and kept free from disease with a standard fungicide regime. Grab samples were taken from each plot at physiological maturity and used to estimate spikes/m<sup>2</sup> and grains/spike. The plots were harvested, grain dried to a constant moisture content, weighed, cleaned and a sub-sample used to estimate thousand grain weight using a Marvin digital seed analyzer (GTA Sensorik). The weighed grain from each plot together with the plot area was used to estimate grain yield in t/ha. Not all lines were in trial for two years and so Best Linear Unbiased Predictors (BLUPs) were calculated for each genotype and trait with the nitrogen treatment as a fixed effect and all others, including the interaction of line with fertilizer, as random effects. BLUPs were generated using the REML directive in Genstat 14 (<http://www.vsni.co.uk/software/genstat/>). All lines were previously genotyped with the barley iSelect 9K SNP platform (Comadran et al., 2012).

#### **Scanning electron microscopy (SEM) analysis**

Immature spikes were fixed in 4% formaldehyde in phosphate buffer. After dehydration and critical point drying, samples were examined in a Hitachi S4100 or a KEYENCE VHX-D510 scanning electron microscope at 5kV acceleration voltage.

#### **Basic mapping**

Five F<sub>2</sub> populations were developed by crossing DZ29 with five different two-rowed accessions (KNG, HN, BO, GP and OUH602). F<sub>2</sub> plants were grown until full maturity under field condition at NIAS, Tsukuba, Japan. To construct a basic genetic map, 78 to 96 plants were used from each of the five F<sub>2</sub> populations. The *deficiens* genotype of F<sub>2</sub> plants was determined by progeny testing 24–30 F<sub>3</sub> plants from each F<sub>2</sub> individual in the field of Central Agricultural Experiment Station, Hokkaido, which enabled classification into the three genotypic classes expected for the segregation of a single Mendelian gene. The length of the lateral florets from the centre of at least three spikes per plant were measured after spike emergence was complete. F<sub>2</sub> individuals were genotyped using selected polymorphic DNA markers from the insertion-deletion (Indel),

single nucleotide polymorphism (SNP), cleaved amplified polymorphic sequence (CAPS) and derived CAPS (dCAPS) markers described by Sakuma et al. (2010). The primers are listed in Table S9 and the resulting genotypic data used to construct linkage maps using MAPMAKER/EXP ver.3.0 (Lander et al., 1987).

### **Fine mapping**

The F<sub>2</sub> segregants of DZ29 × KNG and DZ29 × OUH602 were genotyped with two DNA markers AK376350\_SNP and BC12063\_SNP3 that we found to flank the *deficiens* locus. F<sub>3</sub> progeny in which a recombination had occurred between the two flanking markers were genotyped with *de novo* DNA markers to further delimit the *deficiens* locus (Table S9).

### **Resequencing *Vrs1* in NW European winter barley cultivars**

Genomic DNA was extracted using bench-grown 2 week old leaf tissue with a QIAamp 96 DNA kit on a QIAcube HT automated DNA extraction platform. (Qiagen, Hilden, Germany). DNA quality and quantity was assessed using a NanoDrop 2000 (Thermo Scientific, Massachusetts, USA). PCR amplifications and Sanger sequencing were carried out as described previously (Houston et al., 2012). DNA sequence trimming and alignments were performed using Geneious (vR10, Biomatters Limited, Auckland, NZ). Details of primers used are provided in Table S9.

### **Peptide motif analysis and functional prediction**

To obtain VRS1 homologues from several plant species a BLASTP search (query: BAF43315) was made against the Phytozome v.12.0 (<https://phytozome.jgi.doe.gov/pz/portal.html>) and IPK Barley BLAST Server ([http://webblast.ipk-gatersleben.de/barley\\_ibsc/](http://webblast.ipk-gatersleben.de/barley_ibsc/)). Peptide sequences with a threshold of *E*-value < 1e–10 were retrieved and 87 peptide sequences (Supplementary Data 1) including VRS1 and HvHOX2 (BAI49294) were used for motif analysis. MEME database was used for discovering peptide motifs (Bailey et al., 2006). Prediction of potential phosphorylation amino acid sites was performed using NetPhos 3.1 (Blom et al., 1999; Blom et al., 2004).



532

533 ***In situ* RNA hybridization analysis**

534 Immature spikes at the glume primordium stage and the white anther stage  
535 (Kirby and Appleyard, 1981), from field-grown plants were freshly sampled and  
536 fixed in 4% paraformaldehyde and 0.25% glutaraldehyde in 0.05M  
537 sodium-phosphate buffer pH 7.2. RNA probes of *Vrs1* and *histone H4* were  
538 developed as in Sakuma et al. (2013). Primers are listed in Table S9. *In situ*  
539 hybridization was conducted as described by Komatsuda et al. (2007).

540

541 **RNA extraction and quantitative real-time PCR**

542 Immature spikes were developmentally staged from double ridge stage to yellow  
543 anther stage under a stereoscopic microscope (Kirby and Appleyard, 1981).  
544 Total RNA was extracted from immature spikes, seedling shoots and roots 7  
545 days after germination, leaf blades, leaf sheaths, nodes and internodes at awn  
546 primordium stage using TRIzol (Invitrogen, Carlsbad, CA, USA). RNA was  
547 quantified using a NanoDrop 2000 (Thermo Fisher Scientific, Waltham, MA,  
548 USA). To remove genomic DNA contamination, RNA was treated with  
549 RNase-free DNase (Takara Bio, Tokyo, Japan). First-strand cDNA was  
550 synthesized with SuperScript III (Invitrogen) and first-strand cDNA derived from  
551 20 ng RNA was used as PCR template. Transcript levels of each gene were  
552 measured by qRT-PCR using an ABI Prism 7900HT sequence detection system  
553 (Applied Biosystems, Foster, CA, USA) and THUNDERBIRD SYBR qPCR Mix  
554 Kit (Toyobo, Osaka, Japan) according to the manufacturers' protocols. Primers  
555 used for qRT-PCR are listed in Table S9. qRT-PCR analysis was performed at  
556 least twice for each sample with biological replicates of at least three  
557 independent RNA extractions per sample. Barley *Actin* gene (accession  
558 DN182500) was used to normalize the RNA level for each sample.

559

560 **RNA-seq**

561 Total RNA was extracted from immature spikes at the awn primordium stage of  
562 cv. Foma and a *Deficiens 2* mutant (NGB115174). Total RNA was measured  
563 using an Agilent 2100 Bioanalyzer (Agilent Technologies, Technologies, PaloAlto,

CA, USA) and used for the construction of sequencing libraries. Strand-specific RNA libraries were prepared using the TruSeq Stranded mRNA Sample Prep Kit (Illumina) following the instructions in the TruSeq Stranded mRNA Sample Preparation Guide Rev.E (Illumina). High-throughput sequencing was conducted using a HiSeq 2500 (Table S10, Illumina, San Diego, CA, USA). Sequences were aligned to barley pseudomolecules (Mascher et al. (2017): 160404\_barley\_pseudomolecules\_masked.fasta) with TopHAT2 (Kim et al., 2013). Gene expression was estimated as read counts for each gene locus by featureCounts (Liao et al., 2013) using the gene annotation file Hv\_IBSC\_PGSC\_r1\_HighConf.gtf. Expression levels were normalized by TMM method and *p*-values were calculated by an exact negative binomial test along with the gene-specific variations estimated by empirical Bayes method in edgeR (Robinson et al., 2010). The Benjamini-Hochberg method was applied on the *p*-values to calculate *q*-values and to control the false discovery rate (FDR). Differentially expressed genes (DEGs) were defined as *q*-value < 0.05, *p*-value < 0.05 and log<sub>2</sub> fold change > 1 or < -1. The sequence data have been submitted to the DDBJ Sequence Read Archive under accession number PRJDB4754.

581

### 582 **Gene ontology (GO) term enrichment analysis**

583 GO terms of barley genes were assigned using Arabidopsis GO terms as follows.  
584 *Hordeum vulgare* protein sequences  
585 (160517\_Hv\_IBSC\_PGSC\_r1\_proteins\_HighConf\_REPR\_annotation.fasta)  
586 were compared with the peptide sequence in *Arabidopsis thaliana* (TAIR10;  
587 (Berardini et al., 2015)) using BLAST software (blastp) with a threshold of  
588 *E*-value < 1e-20; (Altschul et al., 1990). GO terms with most similar sequence in  
589 *Arabidopsis* were used as the GO terms of corresponding barley genes. 25,122  
590 barley genes were assigned with more than one GO term (Supplementary Data  
591 2). GO term enrichment analysis of up- (Supplementary Data 3) and  
592 down-regulated genes (Supplementary Data 4) were performed separately using  
593 agriGO (Du et al., 2010) with Fisher's exact test and Benjamini, Hochberg, and  
594 Yekutieli method to control FDR.

595

596 **Haplotype analysis**

597 A haplotype analysis was performed based on re-sequencing data of the *Vrs1*  
598 locus (2062 bp) from 321 domesticated barley accessions and 136 wild barley  
599 accessions (Table S8; Saisho et al., 2009). Sequence alignments were  
600 performed with ClustalW using MEGA7 software (Kumar et al., 2016). A  
601 Median-Joining network (Bandelt et al., 1999) was constructed using the  
602 software programs DNA Alignment v1.3.3.2 and Network v5.0.0.1 (Fluxus  
603 Technology Ltd., Clare, Suffolk, UK) with default parameters (Epsilon=0;  
604 Frequency>1 criterion=inactive; The ratio of transversion:transition=1:1;  
605 Criterion=Connection cost; External rooting=inactive; MJ square  
606 option=inactive).

607  
608 **Accession numbers**

609 The *Vrs1* sequence data have been deposited in DNA Data Bank of Japan  
610 (DDBJ) nucleotide core database under accession numbers LC216328 –  
611 LC216332, except for the NW European cultivars listed in Table S3 which have  
612 been deposited in NCBI under accession numbers MF776900 – MF776946.  
613 . The RNA-seq data have been submitted to the DDBJ Sequence Read Archive  
614 under accession number PRJDB4754.

615  
616 **Acknowledgments**

617 We thank Daisuke Saisho (Okayama University), Naoki Sentoku (NIAS) and  
618 Hiroyuki Tsuji (Yokohama City University) for their help and advice. We are  
619 grateful to Harumi Koyama and Mari Sakuma (NIAS), Corinna Trautewig (IPK),  
620 and Malcolm Macaulay (JHI) for their excellent technical assistance. We thank  
621 Peter Werner, Guillaume Barol-Baron, and David Harrap of KWS UK Ltd for  
622 allowing us to use some of their data from the trials and we also acknowledge  
623 the assistance of Hazel Bull, Richard Keith, and Chris Warden of JHI.

624  
625 **Competing financial interests:**

626 The authors declare no competing financial interests.

627

628 **Figure legends**

629 **Figure 1.** The inflorescence of *deficiens* barley.

630 (A) The morphology of the inflorescence (from left to right: canonical two-rowed  
631 spike cultivar Haruna Nijo, HN; F<sub>1</sub> plant between DZ29 × HN; *deficiens* landrace  
632 Debre Zeit 29, DZ29). Central spikelets of DZ29 are larger than those of HN,  
633 lateral spikelets of DZ29 are smaller than those of HN. (B) Dissected lateral  
634 spikelets. Arrowheads indicate glumes. (C) Variation of floret size in the lateral  
635 spikelet. KNG; Kanto Nakate Gold, GP; Golden Promise. (D–I) SEM images of  
636 two-rowed cultivar Bonus (D, F, H) and DZ29 (E, G, I) at the awn primordium  
637 stage. Asterisks indicate smaller lateral spikelet meristems in DZ29 compared  
638 with Bonus. (J and K) *In situ* mRNA hybridization of *histone H4* shows weaker  
639 expression in lateral spikelet of DZ29 (K) than that of Bonus (J), while stronger  
640 expression in the central spikelet (all the organs) of DZ29 than that of Bonus.  
641 Four serial sections are shown in each cultivar. Scale bars = 1 cm in (A), (B), 500  
642 μm in (D), (E), (J), (K) and 100 μm in (F–I). CS: central spikelet; LS: lateral  
643 spikelet; gl: glume; le: lemma; sm: spikelet meristem.

644  
645 **Figure 2.** Fine mapping of *deficiens* and analysis of induced mutants.

646 (A) The genetic map of the *deficiens* region. The numbers beneath the line  
647 indicate the number of recombinants recovered. One recombination  
648 corresponds to a genetic distance of 0.01 cM. (B) Protein sequence of VRS1.  
649 Independent single amino acid substitutions were identified in DZ29 and induced  
650 mutants (S184G & S187P) at C-terminal region (CTR), respectively. The  
651 Ser-rich motif is highly conserved among plant HD-Zip I proteins (*n* = 87).  
652 Asterisks indicate putative phosphorylation sites. NTR: N-terminal region; HD:  
653 homeodomain; ZIP: leucine zipper. (C) SEM images of Foma (WT) and  
654 *Deficiens 2* (*Def2*) mutant at awn primordium stage. In *Def2* the lateral spikelet  
655 meristem is highly suppressed. CSG: central spikelet glume; LSG: lateral  
656 spikelet glume; LSM: lateral spikelet meristem. (D) Triple spikelet morphology.  
657 (E) Dissected lateral spikelets. Arrowheads indicate glumes. (F) *Def2* mutant  
658 shows bigger grain size. (G–L) Phenotypic comparison between Foma (WT) and  
659 *deficiens* mutants. (G) Floret length in the lateral spikelet. (H) Grain length. (I)

660 Grain width. (J) Central spikelet number per spike. (K) Plant height (L) Spike  
661 number per plant. Data are given as mean  $\pm$  sd ( $n = 20$ ). \*\*, \*, Means are  
662 significantly different at the 1 and 5% probability levels, respectively; ns, not  
663 significantly different. Scale bars show 100  $\mu$ m in (C) and 1 cm in (D–F).

664  
665 **Figure 3.** Mean effect of *deficiens* allele for grain yield.

666 (A) Thousand grain weight (TGW). (B) Grains per ear. (C) Spikes per m<sup>2</sup>. (D)  
667 Yield (t/ha). Data were obtained from 5 site/seasons field trial of 24 two-rowed  
668 and 24 *deficiens* NW European cultivars grown under a winter feed barley  
669 regime (200kg total N/ha). \*\*, \*, Means are significantly different at the 1 and 5%  
670 probability levels, respectively; ns, not significantly different.

671  
672 **Figure 4.** Transcript pattern of *Vrs1*, *Vrs4* and *HvHox2*.

673 (A–C) Quantitative real time PCR comparison of *Vrs1* (A), *Vrs4* (B), and *HvHox2*  
674 (C) in selected tissues between Foma and *Deficiens 2* mutant. DR: double ridge  
675 stage; TM: triple-mound stage; GP: glume primordium stage; LP: lemma  
676 primordium stage; SP: stamen primordium stage; AP: awn primordium stage;  
677 WA: white anther stage; GA: green anther stage; YA: yellow anther stage; SH:  
678 shoots; RO: roots; LB: leaf blade; LS: leaf sheath; NO: nodes; IN: internodes.  
679 (D–G) *In situ* mRNA hybridization with *Vrs1* antisense probe. *Vrs1* is  
680 predominantly expressed in the lateral spikelet meristem at the glume  
681 primordium stage of Bonus (*Vrs1.b3*, D) and DZ29 (*Vrs1.t1*, E). At the white  
682 anther stage, *Vrs1* is mainly localized in lemma, pistil and rachilla in Bonus (F)  
683 whereas *Vrs1* is expressed in floret meristem and lemma primordia in DZ29 (G).  
684 Cs: central spikelet; Ls: lateral spikelet; Gl: glume; Le: lemma; St: stamen; Pi:  
685 pistil; Ra: rachilla. Scale bars show 200  $\mu$ m.

686  
687 **Figure 5.** Transcriptional regulation by the *Deficiens* mutation.

688 (A) Heat map of differentially expressed genes (DEG) in *Def2* mutant (*Vrs1.t2*  
689 allele) compared with Foma. (B) Hierarchical tree graph of Gene Ontology (GO)  
690 enrichment for the up-regulated DEG. Numbers in parentheses indicate *q*-values.  
691 Solid, dashed, and dotted lines represent two, one and zero enriched terms at

692 both ends connected by the line, respectively.

693

694 **Figure 6.** Haplotype network analysis of *Vrs1*.

695 Median-Joining network was constructed from the haplotypes based on the  
696 re-sequencing of 321 domesticated and 136 wild barley accessions. Circle sizes  
697 correspond to the frequency of individual haplotypes. Lines represent genetic  
698 distances between haplotypes. Open circle indicate inferred intermediate  
699 haplotypes.

700

#### 701 **Supplemental Material**

702 **Table S1.** Segregation analysis of *deficiens* in five F2 mapping populations.

703 **Table S2.** The mapping population used for fine mapping of *deficiens*.

704 **Table S3.** *Vrs1* sequence information of *deficiens* barley.

705 **Table S4.** List of *Deficiens* and *Semi-deficiens* mutants with description of  
706 mutational events in *Vrs1*.

707 **Table S5.** Motif analysis of HD-Zip I transcription factor in plants (n = 87).

708 **Table S6.** Differentially regulated genes in *Deficiens2* mutants compared to  
709 wild-type.

710 **Table S7.** Gene Ontology (GO) enrichment analysis for up-regulated  
711 differentially expressed genes in *Deficiens 2* mutant.

712 **Table S8.** Haplotype information of 321 domesticated and 136 wild barley.

713 **Table S9.** Primer information used in this study.

714 **Table S10.** Summary of RNA-sequence experiment.

715

716 **Fig. S1.** Summary of the tonnes of certified seed production each year in UK.

717 **Fig. S2.** Additional replicates of the RNA *in situ* hybridization of *histone H4*.

718 **Fig. S3.** Frequency distributions of floret length in the lateral spikelet.

719 **Fig. S4.** Comparative basic genetic maps of *deficiens* on chromosome 2H.

720 **Fig. S5.** Alignment of deduced amino acid sequences of VRS1.

721 **Fig. S6.** Spike phenotype of *deficiens* mutants.

722 **Fig. S7.** Representation of motifs in VRS1 homologs.

723 **Fig. S8.** Scanning electron microscopy views of barley spikes.

724 **Fig. S9.** Predicted phosphorylation sites of Serine in VRS1 protein.  
725 **Fig. S10.** Expression pattern of *Vrs1* and *HvHox2* in Debre Zeit 29.  
726  
727 **Supplementary Data 1.** Peptide sequences used for motif analysis.  
728 **Supplementary Data 2.** GO terms of 25,122 barley genes.  
729 **Supplementary Data 3.** GO terms of up-regulated genes.  
730 **Supplementary Data 4.** GO terms of down-regulated genes.





## Parsed Citations

**Altschul SF, Gish W, Miller W, Myers EW, Lipman DJ (1990)** Basic local alignment search tool. *J Mol Biol* 215: 403-410

Pubmed: [Author and Title](#)

CrossRef: [Author and Title](#)

Google Scholar: [Author Only](#) [Title Only](#) [Author and Title](#)

**Arce AL, Raineri J, Capella M, Cabello JV, Chan RL (2011)** Uncharacterized conserved motifs outside the HD-Zip domain in HD-Zip subfamily I transcription factors; a potential source of functional diversity. *BMC Plant Biol* 11: 42

Pubmed: [Author and Title](#)

CrossRef: [Author and Title](#)

Google Scholar: [Author Only](#) [Title Only](#) [Author and Title](#)

**Ariel FD, Manavella PA, Dezar CA, Chan RL (2007)** The true story of the HD-Zip family. *Trends Plant Sci* 12: 419-426

Pubmed: [Author and Title](#)

CrossRef: [Author and Title](#)

Google Scholar: [Author Only](#) [Title Only](#) [Author and Title](#)

**Ashikari M, et al. (2005)** Cytokinin oxidase regulates rice grain production. *Science* 309: 741-745

Pubmed: [Author and Title](#)

CrossRef: [Author and Title](#)

Google Scholar: [Author Only](#) [Title Only](#) [Author and Title](#)

**Bailey TL, Williams N, Misleh C, Li WW (2006)** MEME: discovering and analyzing DNA and protein sequence motifs. *Nucleic Acids Res* 34: W369-373

Pubmed: [Author and Title](#)

CrossRef: [Author and Title](#)

Google Scholar: [Author Only](#) [Title Only](#) [Author and Title](#)

**Bandelt HJ, Forster P, Rohl A (1999)** Median-joining networks for inferring intraspecific phylogenies. *Mol Biol Evol* 16: 37-48

Pubmed: [Author and Title](#)

CrossRef: [Author and Title](#)

Google Scholar: [Author Only](#) [Title Only](#) [Author and Title](#)

**Berardini TZ, Reiser L, Li D, Mezheritsky Y, Muller R, Strait E, Huala E (2015)** The Arabidopsis information resource: Making and mining the "gold standard" annotated reference plant genome. *Genesis* 53: 474-485

Pubmed: [Author and Title](#)

CrossRef: [Author and Title](#)

Google Scholar: [Author Only](#) [Title Only](#) [Author and Title](#)

**Blom N, Gammeltoft S, Brunak S (1999)** Sequence and structure-based prediction of eukaryotic protein phosphorylation sites. *J Mol Biol* 294: 1351-1362

Pubmed: [Author and Title](#)

CrossRef: [Author and Title](#)

Google Scholar: [Author Only](#) [Title Only](#) [Author and Title](#)

**Blom N, Sicheritz-Ponten T, Gupta R, Gammeltoft S, Brunak S (2004)** Prediction of post-translational glycosylation and phosphorylation of proteins from the amino acid sequence. *Proteomics* 4: 1633-1649

Pubmed: [Author and Title](#)

CrossRef: [Author and Title](#)

Google Scholar: [Author Only](#) [Title Only](#) [Author and Title](#)

**Bommert P, Nagasawa NS, Jackson D (2013)** Quantitative variation in maize kernel row number is controlled by the FASCIATED EAR2 locus. *Nat Genet*

Pubmed: [Author and Title](#)

CrossRef: [Author and Title](#)

Google Scholar: [Author Only](#) [Title Only](#) [Author and Title](#)

**Bothmer R, Jacobsen N, Baden C, Jorgensen R, Linde-Laursen I (1995)** An ecogeographical study of the genus *Hordeum*, Ed 2nd. IBPGR, Rome

Pubmed: [Author and Title](#)

CrossRef: [Author and Title](#)

Google Scholar: [Author Only](#) [Title Only](#) [Author and Title](#)

**Bull H, et al. (2017)** Barley SIX-ROWED SPIKE3 encodes a putative Jumonji C-type H3K9me2/me3 demethylase that represses lateral spikelet fertility. *Nat Commun*

Pubmed: [Author and Title](#)

CrossRef: [Author and Title](#)

Google Scholar: [Author Only](#) [Title Only](#) [Author and Title](#)

**Comadran J, et al. (2012)** Natural variation in a homolog of *Antirrhinum* CENTRORADIALIS contributed to spring growth habit and environmental adaptation in cultivated barley. *Nat Genet*

Pubmed: [Author and Title](#)

CrossRef: [Author and Title](#)

Google Scholar: [Author Only](#) [Title Only](#) [Author and Title](#)

**Doebley JF, Gaut BS, Smith BD (2006) The molecular genetics of crop domestication. Cell 127: 1309-1321**

Pubmed: [Author and Title](#)

CrossRef: [Author and Title](#)

Google Scholar: [Author Only](#) [Title Only](#) [Author and Title](#)

**Druka A, et al. (2011) Genetic dissection of barley morphology and development. Plant Physiol 155: 617-627**

Pubmed: [Author and Title](#)

CrossRef: [Author and Title](#)

Google Scholar: [Author Only](#) [Title Only](#) [Author and Title](#)

**Du Z, Zhou X, Ling Y, Zhang Z, Su Z (2010) agriGO: a GO analysis toolkit for the agricultural community. Nucleic Acids Res 38: W64-70**

Pubmed: [Author and Title](#)

CrossRef: [Author and Title](#)

Google Scholar: [Author Only](#) [Title Only](#) [Author and Title](#)

**Fujiwara S, Wang L, Han L, Suh SS, Salome PA, McClung CR, Somers DE (2008) Post-translational regulation of the Arabidopsis circadian clock through selective proteolysis and phosphorylation of pseudo-response regulator proteins. J Biol Chem 283: 23073-23083**

Pubmed: [Author and Title](#)

CrossRef: [Author and Title](#)

Google Scholar: [Author Only](#) [Title Only](#) [Author and Title](#)

**Habgood RM, Chambi JY (1984) Effects of the deficiens allele on ear development and yield in barley. Annals of Applied Biology 105: 159-166**

Pubmed: [Author and Title](#)

CrossRef: [Author and Title](#)

Google Scholar: [Author Only](#) [Title Only](#) [Author and Title](#)

**Han Y, Zhang C, Yang H, Jiao Y (2014) Cytokinin pathway mediates APETALA1 function in the establishment of determinate floral meristems in Arabidopsis. Proc Natl Acad Sci U S A 111: 6840-6845**

Pubmed: [Author and Title](#)

CrossRef: [Author and Title](#)

Google Scholar: [Author Only](#) [Title Only](#) [Author and Title](#)

**Houston K, Druka A, Bonar N, Macaulay M, Lundqvist U, Franckowiak J, Morgante M, Stein N, Waugh R (2012) Analysis of the barley bract suppression gene Trd1. Theor Appl Genet 125: 33-45**

Pubmed: [Author and Title](#)

CrossRef: [Author and Title](#)

Google Scholar: [Author Only](#) [Title Only](#) [Author and Title](#)

**Hua L, et al. (2015) LABA1, a Domestication Gene Associated with Long, Barbed Awns in Wild Rice. Plant Cell 27: 1875-1888**

Pubmed: [Author and Title](#)

CrossRef: [Author and Title](#)

Google Scholar: [Author Only](#) [Title Only](#) [Author and Title](#)

**Hunter T, Karin M (1992) The regulation of transcription by phosphorylation. Cell 70: 375-387**

Pubmed: [Author and Title](#)

CrossRef: [Author and Title](#)

Google Scholar: [Author Only](#) [Title Only](#) [Author and Title](#)

**Kim D, Pertea G, Trapnell C, Pimentel H, Kelley R, Salzberg SL (2013) TopHat2: accurate alignment of transcriptomes in the presence of insertions, deletions and gene fusions. Genome Biol 14: R36**

Pubmed: [Author and Title](#)

CrossRef: [Author and Title](#)

Google Scholar: [Author Only](#) [Title Only](#) [Author and Title](#)

**Kirby EJM, Appleyard M (1981) Cereal development guide, Ed 1st. Cereal Unit, Kenilworth**

Pubmed: [Author and Title](#)

CrossRef: [Author and Title](#)

Google Scholar: [Author Only](#) [Title Only](#) [Author and Title](#)

**Komatsuda T, et al. (2007) Six-rowed barley originated from a mutation in a homeodomain-leucine zipper I-class homeobox gene. Proc Natl Acad Sci U S A 104: 1424-1429**

Pubmed: [Author and Title](#)

CrossRef: [Author and Title](#)

Google Scholar: [Author Only](#) [Title Only](#) [Author and Title](#)

**Koppolu R, et al. (2013) Six-rowed spike4 (Vrs4) controls spikelet determinacy and row-type in barley. Proc Natl Acad Sci U S A 110: 13198-13203**

Pubmed: [Author and Title](#)

CrossRef: [Author and Title](#)

Google Scholar: [Author Only](#) [Title Only](#) [Author and Title](#)

**Kumar S, Stecher G, Tamura K (2016) MEGA7: Molecular Evolutionary Genetics Analysis Version 7.0 for Bigger Datasets. Mol Biol Evol 33: 1870-1874**

Pubmed: [Author and Title](#)  
CrossRef: [Author and Title](#)  
Google Scholar: [Author Only](#) [Title Only](#) [Author and Title](#)

**Lander ES, Green P, Abrahamson J, Barlow A, Daly MJ, Lincoln SE, Newberg LA (1987) MAPMAKER: an interactive computer package for constructing primary genetic linkage maps of experimental and natural populations. Genomics 1: 174-181**

Pubmed: [Author and Title](#)  
CrossRef: [Author and Title](#)  
Google Scholar: [Author Only](#) [Title Only](#) [Author and Title](#)

**Li Y, et al. (2011) Natural variation in GS5 plays an important role in regulating grain size and yield in rice. Nat Genet 43: 1266-1269**

Pubmed: [Author and Title](#)  
CrossRef: [Author and Title](#)  
Google Scholar: [Author Only](#) [Title Only](#) [Author and Title](#)

**Liao Y, Smyth GK, Shi W (2013) The Subread aligner: fast, accurate and scalable read mapping by seed-and-vote. Nucleic Acids Res 41: e108**

Pubmed: [Author and Title](#)  
CrossRef: [Author and Title](#)  
Google Scholar: [Author Only](#) [Title Only](#) [Author and Title](#)

**Luo J, et al. (2013) An-1 encodes a basic helix-loop-helix protein that regulates awn development, grain size, and grain number in rice. Plant Cell 25: 3360-3376**

Pubmed: [Author and Title](#)  
CrossRef: [Author and Title](#)  
Google Scholar: [Author Only](#) [Title Only](#) [Author and Title](#)

**Mascher M, et al. (2017) A chromosome conformation capture ordered sequence of the barley genome. Nature 544: 427-433**

Pubmed: [Author and Title](#)  
CrossRef: [Author and Title](#)  
Google Scholar: [Author Only](#) [Title Only](#) [Author and Title](#)

**Poursarebani N, et al. (2015) The Genetic Basis of Composite Spike Form in Barley and 'Miracle-Wheat'. Genetics 201: 155-165**

Pubmed: [Author and Title](#)  
CrossRef: [Author and Title](#)  
Google Scholar: [Author Only](#) [Title Only](#) [Author and Title](#)

**Powers L (1936) The Nature of the Interaction of Genes Affecting Four Quantitative Characters in a Cross between Hordeum Deficiens and Hordeum Vulgare. Genetics 21: 398-420**

Pubmed: [Author and Title](#)  
CrossRef: [Author and Title](#)  
Google Scholar: [Author Only](#) [Title Only](#) [Author and Title](#)

**Ramsay L, et al. (2011) INTERMEDIUM-C, a modifier of lateral spikelet fertility in barley, is an ortholog of the maize domestication gene TEOSINTE BRANCHED 1. Nat Genet 43: 169-172**

Pubmed: [Author and Title](#)  
CrossRef: [Author and Title](#)  
Google Scholar: [Author Only](#) [Title Only](#) [Author and Title](#)

**Robinson MD, McCarthy DJ, Smyth GK (2010) edgeR: a Bioconductor package for differential expression analysis of digital gene expression data. Bioinformatics 26: 139-140**

Pubmed: [Author and Title](#)  
CrossRef: [Author and Title](#)  
Google Scholar: [Author Only](#) [Title Only](#) [Author and Title](#)

**Saisho D, Pourkheirandish M, Kanamori H, Matsumoto T, Komatsuda T (2009) Allelic variation of row type gene Vrs1 in barley and implication of the functional divergence. Breed Sci 59: 621-628**

Pubmed: [Author and Title](#)  
CrossRef: [Author and Title](#)  
Google Scholar: [Author Only](#) [Title Only](#) [Author and Title](#)

**Sakuma S, et al. (2013) Divergence of expression pattern contributed to neofunctionalization of duplicated HD-Zip I transcription factor in barley. New Phytol 197: 939-948**

Pubmed: [Author and Title](#)  
CrossRef: [Author and Title](#)  
Google Scholar: [Author Only](#) [Title Only](#) [Author and Title](#)

**Sakuma S, Pourkheirandish M, Matsumoto T, Koba T, Komatsuda T (2010) Duplication of a well-conserved homeodomain-leucine zipper transcription factor gene in barley generates a copy with more specific functions. Funct Integr Genomics 10: 123-133**

Pubmed: [Author and Title](#)  
CrossRef: [Author and Title](#)  
Google Scholar: [Author Only](#) [Title Only](#) [Author and Title](#)

**Sarid-Krebs L, Panigrahi KC, Fornara F, Takahashi Y, Hayama R, Jang S, Tilmes V, Valverde F, Coupland G (2015) Phosphorylation of CONSTANS and its COP1-dependent degradation during photoperiodic flowering of Arabidopsis. Plant J 84: 451-463**

Pubmed: [Author and Title](#)  
Downloaded from on November 9, 2017 - Published by www.plantphysiol.org  
Copyright © 2017 American Society of Plant Biologists. All rights reserved.

CrossRef: [Author and Title](#)  
Google Scholar: [Author Only](#) [Title Only](#) [Author and Title](#)

**Shomura A, Izawa T, Ebana K, Ebitani T, Kanegae H, Konishi S, Yano M (2008) Deletion in a gene associated with grain size increased yields during rice domestication. Nat Genet 40: 1023-1028**

Pubmed: [Author and Title](#)  
CrossRef: [Author and Title](#)  
Google Scholar: [Author Only](#) [Title Only](#) [Author and Title](#)

**Simmonds J, Scott P, Brinton J, Mestre TC, Bush M, Del Blanco A, Dubcovsky J, Uauy C (2016) A splice acceptor site mutation in TaGW2-A1 increases thousand grain weight in tetraploid and hexaploid wheat through wider and longer grains. Theor Appl Genet 129: 1099-1112**

Pubmed: [Author and Title](#)  
CrossRef: [Author and Title](#)  
Google Scholar: [Author Only](#) [Title Only](#) [Author and Title](#)

**Song XJ, Huang W, Shi M, Zhu MZ, Lin HX (2007) A QTL for rice grain width and weight encodes a previously unknown RING-type E3 ubiquitin ligase. Nat Genet 39: 623-630**

Pubmed: [Author and Title](#)  
CrossRef: [Author and Title](#)  
Google Scholar: [Author Only](#) [Title Only](#) [Author and Title](#)

**Song XJ, et al. (2015) Rare allele of a previously unidentified histone H4 acetyltransferase enhances grain weight, yield, and plant biomass in rice. Proc Natl Acad Sci U S A 112: 76-81**

Pubmed: [Author and Title](#)  
CrossRef: [Author and Title](#)  
Google Scholar: [Author Only](#) [Title Only](#) [Author and Title](#)

**Studer A, Zhao Q, Ross-Ibarra J, Doebley J (2011) Identification of a functional transposon insertion in the maize domestication gene tb1. Nat Genet 43: 1160-1163**

Pubmed: [Author and Title](#)  
CrossRef: [Author and Title](#)  
Google Scholar: [Author Only](#) [Title Only](#) [Author and Title](#)

**Sugiyama N, Nakagami H, Mochida K, Daudi A, Tomita M, Shirasu K, Ishihama Y (2008) Large-scale phosphorylation mapping reveals the extent of tyrosine phosphorylation in Arabidopsis. Mol Syst Biol 4: 193**

Pubmed: [Author and Title](#)  
CrossRef: [Author and Title](#)  
Google Scholar: [Author Only](#) [Title Only](#) [Author and Title](#)

**van Esse GW, Walla A, Finke A, Koornneef M, Pecinka A, von Korff M (2017) Six-Rowed Spike3 (VRS3) Is a Histone Demethylase That Controls Lateral Spikelet Development in Barley. Plant Physiol 174: 2397-2408**

Pubmed: [Author and Title](#)  
CrossRef: [Author and Title](#)  
Google Scholar: [Author Only](#) [Title Only](#) [Author and Title](#)

**Wang S, et al. (2012) Control of grain size, shape and quality by OsSPL16 in rice. Nat Genet 44: 950-954**

Pubmed: [Author and Title](#)  
CrossRef: [Author and Title](#)  
Google Scholar: [Author Only](#) [Title Only](#) [Author and Title](#)

**Wendt T, Holmø I, Dockter C, Preuss A, Thomas W, Druka A, Waugh R, Hansson M, Braumann I (2016) HvDep1 Is a Positive Regulator of Culm Elongation and Grain Size in Barley and Impacts Yield in an Environment-Dependent Manner. PLoS One 11: e0168924**

Pubmed: [Author and Title](#)  
CrossRef: [Author and Title](#)  
Google Scholar: [Author Only](#) [Title Only](#) [Author and Title](#)

**Woodward RW (1947) The lh, l, i alleles in Hordeum deficiens genotypes of barley. J. Am. Soc. Agron. 39: 474-482**

Pubmed: [Author and Title](#)  
CrossRef: [Author and Title](#)  
Google Scholar: [Author Only](#) [Title Only](#) [Author and Title](#)

**Woodward RW (1949) The inheritance of fertility in the lateral florets of the four barley groups. Agron J. 41: 317-322**

Pubmed: [Author and Title](#)  
CrossRef: [Author and Title](#)  
Google Scholar: [Author Only](#) [Title Only](#) [Author and Title](#)

**Youssef HM, et al. (2017) VRS2 regulates hormone-mediated inflorescence patterning in barley. Nat Genet 49: 157-161**

Pubmed: [Author and Title](#)  
CrossRef: [Author and Title](#)  
Google Scholar: [Author Only](#) [Title Only](#) [Author and Title](#)

**Youssef HM, Koppolu R, Rutten T, Korzun V, Schweizer P, Schnurbusch T (2014) Genetic mapping of the labile (lab) gene: a recessive locus causing irregular spikelet fertility in labile-barley (Hordeum vulgare convar. labile). Theor Appl Genet 127: 1123-1131**

Pubmed: [Author and Title](#)  
CrossRef: [Author and Title](#)

